ASTRONOMY & ASTROPHYSICS
SUPPLEMENT SERIES

Astron. Astrophys. Suppl. Ser. **135**, 273–289 (1999)

Gigahertz Peaked Spectrum sources from the Jodrell Bank–VLA Astrometric Survey

I. Sources in the region $35° \leq \delta \leq 75°$

A. Marecki[1], **H. Falcke**[2], **J. Niezgoda**[1], **S.T. Garrington**[3], **and A.R. Patnaik**[2]

[1] Centre for Astronomy, N. Copernicus University, ul. Gagarina 11, PL-87-100 Toruń, Poland
[2] Max-Planck-Institut für Radioastronomie, Auf dem Hügel 69, D-53121 Bonn, Germany
[3] Nuffield Radio Astronomy Laboratories, Jodrell Bank, Cheshire, SK11 9DL, UK

Received May 14; accepted October 13, 1998

Abstract. Observations with MERLIN[1] at 408 MHz have been used to establish the low-frequency part of the spectra of more than a hundred compact radio sources taken from the part of the Jodrell Bank–VLA Astrometric Survey limited by $35° \leq \delta \leq 75°$. These sources were selected from JVAS and other catalogues to have convex spectra between 1.4 and 8.4 GHz, characteristic of Gigahertz Peaked Spectrum (GPS) sources. We have confirmed convex shapes of the spectra of 76 objects (one half of our initial candidates) thereby yielding the largest genuine sample of GPS sources compiled so far. Seven of 17 identified quasars in the sample have large ($z \gtrsim 2$) redshifts.

Key words: catalogs — galaxies: active — quasars: general — radio continuum: general

1. Introduction

By definition, Gigahertz Peaked Spectrum (GPS) sources have convex spectra with a turnover frequency $\nu_{\max} > 1$ GHz. It is generally accepted that such a spectral shape results from synchrotron self-absorption due to a high compactness. Indeed, the linear sizes of GPS sources are very small ($10 - 1000$ pc) and their radio luminosities are large ($L_{\rm radio} \sim 10^{45}$ erg/s). An important feature which makes the GPS class particularly interesting, is that GPS objects identified with quasars often have very large redshifts. A review on the properties of GPS sources has been given by O'Dea et al. (1991) — hereinafter OBS91 — and O'Dea (1998). De Vries et al. (1997) compiled spectra of 72 GPS sources and constructed a canonical GPS radio spectrum. They found it to have a constant shape independent of AGN type, redshift or radio luminosity.

As Gopal-Krishna & Spoelstra (1993) pointed out, *the great potential of GPS sources for discovering high-z objects continues to be the major motivation factor for enlarging the sample of GPS sources.* A second motivation for increasing the number of known GPS sources comes from the discovery (Wilkinson et al. 1994) of a new class of Compact Symmetric Objects (CSO). Five archetypal CSOs (cf. Readhead et al. 1996a) are all acknowledged GPS sources. Readhead et al. (1996b) argue that CSOs are the young precursors of classical double radio sources. Increasing the list of known GPS sources offers a promising way to find more CSOs.

The search for GPS sources can be difficult because it requires both high resolution and high sensitivity observations at frequencies well below 1 GHz and high sensitivity observations at $\nu > 5$ GHz, well above the potential peak of the spectrum. Therefore, unlike in the case of flat spectrum sources, only a modest number of GPS sources can simply be extracted from classical large catalogues e.g. the Green Bank (GB) surveys at 1.4 GHz and 4.85 GHz (White & Becker 1992 and references therein — hereinafter WB92) and the Texas Survey at 365 MHz (Douglas et al. 1996). For example, the sample of Stanghellini et al. (1990) was derived from the Texas Survey and the 1 Jy catalogue of Kühr et al. (1981a). Out of 55 sources and candidates they listed, 41 are currently acknowledged as GPS sources (O'Dea, priv. comm. 1996) and 33 make a complete sample (Stanghellini et al. 1996).

The lists published by Gopal-Krishna et al. (1983) and Spoelstra et al. (1985) resulting from dedicated observations, e.g. with the Westerbork Synthesis Radio Telescope

Send offprint requests to: H. Falcke,
e-mail: hfalcke@mpifr-bonn.mpg.de

[1] MERLIN is operated by The University of Manchester on behalf of the UK Particle Physics and Astronomy Research Council.

(WSRT) or the Ooty telescope, are not very large: each one contains 25 sources (5 and 2 out of these two samples respectively had been retracted later). The sources gathered by the authors mentioned above have been collected in OBS91 in the so called "working sample" encompassing 95 objects. Gopal-Krishna & Spoelstra (1993) confirmed the existence of 10 GPS sources and Cersosimo et al. (1994) found 7 more[2]. On the other hand 6 sources from the list in OBS91, namely 0218+357, 0528+134, 0902+490, 1851+488, 2053−201 and 2230+114 proved to be "not so good" examples of the class and have been retracted. By the end of 1997 very few other GPS sources had been discovered.

There are two ways to achieve a "bulk" increase of this number. The first one has been followed by Snellen et al. (1998) — hereinafter SSB98 — the second is the basis of this paper. The former one is based on the Westerbork Northern Sky Survey (WENSS) being carried out with WSRT at 325 and 609 MHz. Naturally, the sources with inverted spectra in the WENSS are GPS candidates, which are followed up with observations at higher frequencies. This survey is particularly useful since it is the most sensitive survey at low frequencies (more than an order of magnitude better than the Texas Survey).

The published part of WENSS called "mini–survey" (Rengelink et al. 1997) is limited to $14^{\rm h}10^{\rm m} < \alpha < 20^{\rm h}30^{\rm m}$, $57^\circ < \delta < 72^\circ50'$ and covers ∼570 square degrees only, so there are still large parts of the sky where this method cannot be applied. Nevertheless, SSB98 using the mini–survey plus an unpublished part of WENSS ($4^{\rm h} < \alpha < 8^{\rm h}30^{\rm m}$, the same declination range as the mini–survey) were able to establish a list of 47 "new" GPS sources.

2. Construction of the sample

Since WENSS was not available when our programme started in 1994, we adopted a different approach which can be regarded as "opposite" to that of SSB98 because we started at the high frequencies end instead of the low one. Hence, to determine candidate GPS sources, we used 8.4 GHz fluxes from the first part of the Jodrell Bank–VLA Astrometric Survey (JVAS)[3] (Patnaik et al. 1992) containing all compact radio sources in the range $35^\circ \le \delta \le 75^\circ$ with fluxes > 200 mJy at 5 GHz. We combined them with 1.4 GHz and 4.85 GHz fluxes from the GB catalogues (WB92). For 32 sources 1.4 GHz fluxes were missing in WB92 so we substituted them with the catalogue flux density limit. Then we fitted the data with a second order polynomial of the form:

$$\log S_\nu = S_0 + \alpha \log \nu - c(\log \nu)^2, \quad (1)$$

where ν is the observed frequency in GHz and S_ν the flux density in mJy and selected the sources with convex spectral shapes. The criterion for selecting an initial list of candidate GPS sources was that the curvature c had to be greater than 1 with a peak in the spectrum in the observable range (the limit of $c > 1$ is rather conservative and includes also spectra which are much flatter than those of typical GPS sources). Admittedly, although this criterion seems to be conservative enough, a few sources from the OBS91 "working sample" which happen to be JVAS members, and therefore have been fitted with polynomials (0018+729, 0248+430, 0552+398, 2015+657, 2021+614, 2352+495), *did not* fulfill it. In the end, the $c > 1$ threshold was chosen as a good compromise, to produce a reasonably sized sample for future observations.

Table 1. Subsample One

IAUname (B1950)	R.A. (J2000)	Dec.	Opt. ID
0059+581	01 02 45.7630	58 24 11.139	CW
0102+480	01 05 49.9295	48 19 03.183	EF
0627+532	06 31 34.6860	53 11 27.754	BS
0652+426	06 56 10.6629	42 37 02.751	G
0652+577	06 57 12.5027	57 41 56.740	EF
0750+535	07 54 15.2177	53 24 56.450	EF
0828+493	08 32 23.2171	49 13 21.036	BL
1107+485	11 10 36.3237	48 17 52.446	EF
1239+552	12 41 27.7043	54 58 19.040	EF
1256+546	12 58 15.6078	54 21 52.112	EF
1311+552	13 13 37.8518	54 58 23.894	EF
1428+422	14 30 23.7418	42 04 36.503	EF
1532+680	15 32 43.3426	67 55 13.992	EF
1602+576	16 03 55.9311	57 30 54.415	BS
1627+476	16 28 37.5064	47 34 10.414	BS
1630+358	16 32 31.2578	35 47 37.740	EF
1745+670	17 45 54.3577	67 03 49.302	EF
1755+578	17 56 03.6285	57 48 47.990	BS
1815+614	18 15 36.7920	61 27 11.641	EF
1946+708	19 45 53.5197	70 55 48.723	?
2253+417	22 55 36.7082	42 02 52.535	BS
2310+385	23 12 58.7950	38 47 42.668	BS
2323+478	23 25 44.9131	48 06 25.280	BS
2356+385	23 59 33.1809	38 50 42.322	BS

Explanation of ID field:

BL: BL Lac object
BS: blue stell. obj. (without the spec. - basically a quasar)
BG: blue galaxy?
CW: crowded field - too many objects for a clean identification
EF: empty field
G: galaxy
NS: neutral stell. obj. (same magn. in both E and O prints)
OB: obscured field
Q: quasar
RS: red stellar object.

[2] Cersosimo et al. claim to discover more sources but only 7 have been finally recognised as GPS.

[3] JVAS resulted from observations made with the VLA in "A" configuration.

The number of the initial candidates selected with the above procedure was 163.

This list contained 14 known GPS sources: 0108+388, 0153+744, 0636+680, 0646+600, 0710+439, 0711+356, 1031+567, 1225+368, 1333+459, 1843+356 and 2050+364 listed in OBS91; 0903+684 from Gopal-Krishna & Spoelstra (1993) and two discovered by Snellen et al. (1995) — 0700+470 and 1324+574. These were not considered for further observations.

We divided the remaining sample of 149 sources into two parts. The first one — hereinafter "Subsample One" — contains those which are found in the 365 MHz Texas survey (24 sources). They are listed in Table 1 along with JVAS positions rounded to 1 milliarcsecond and our identifications made using POSS. Nine of these are also listed in the 6C catalogue which has a flux density limit of 200 mJy at 151 MHz (Hales et al. 1993 and references therein).

For the remaining 125 sources — hereinafter "Subsample Two" — we had virtually no low frequency data. Although 19 of these sources were present in the B3 survey at 408 MHz (Ficarra et al. 1985), its overlap in sky coverage with the first part of the JVAS survey we use here is small and, furthermore, the B3 survey has significant errors in flux density near the catalogue limit of 100 mJy.

The aforementioned crude extrapolation of the spectra applied to medium and high frequency data (1.4 GHz $< \nu <$ 8.4 GHz) of Subsample Two plus the flux density limit of the Texas Survey gave us only an unreliable estimate of the frequency turnover and even the convex shape of the spectrum remained uncertain in some cases. Particularly some weaker sources could either be GPS or mere flat spectrum depending on whether their 365 MHz fluxes were far below or *just* below the Texas catalogue limit respectively. Another effect that will produce a spurious convex shape in our non-simultaneous data is the variability typically observed in flat spectrum sources.

3. Observations and data reduction

In order to investigate the low frequency part of the spectra of Subsample Two sources we set up a programme of flux density measurements at low frequency with a high resolution facility. We used MERLIN at 408 MHz because of its superior resolving capability — 1″. The observations were carried out in the period from November 1994 until January 1995 and each source was typically observed twice (with different hour angles) for about 15 minutes per scan.

Such short snapshots cannot be used to produce reliable maps with MERLIN, since the aperture coverage is too sparse. Confusion is a significant effect at this low frequency and therefore fringe-frequency vs. delay (FFD) plots were used to separate confusing sources from the central target source (see e.g. Walker 1981). Since the data were not phase-calibrated the coherence time is limited to a few minutes. By taking 128×4 second sub-samples of the data and Fourier transforming them in both time and frequency, a "map" of the field surrounding the source can be produced whose axes are fringe-frequency and delay. The target source will have close to zero fringe-frequency and delay, since its position is well known from the JVAS survey, and appear at the centre of the "map", while confusing sources will be offset from the centre. The flux density of the target source was determined from the central peak in the FFD map. The FFD plots were inspected visually; the detection threshold in a single plot was set at 3σ and flux density values were only listed if the target was detected in two or more plots. In all cases, the values determined from the FFD plots were consistent with simple averages of phase-calibrated data on individual baselines calculated using the Astronomical Image Processing System (AIPS). The flux density scale was determined using observations of 3C 286, for which the Baars et al. (1977) value was used.

In Table 2 we report the results of successful measurements of 408 MHz fluxes for 98 sources from Subsample Two along with their JVAS positions rounded to 1 milliarcsecond and our identifications made using POSS. Interference and other problems at other sites resulted in the loss of data for the remaining 27 sources. They are listed in Table 3. The flux density values given in Table 2 resulted from averaging the measurements over all baselines involving the Defford or Knockin telescopes (6 or 8 baselines, depending on whether the Lovell telescope was used or not) and in both LL and RR polarisations. Shorter baselines were not used because they provide insufficient resolution in delay or fringe-frequency to separate the confusing sources; additionally the use of longer baselines reduces any contribution from large-scale halos seen around some GPS sources. The longest baselines involving the Cambridge telescope were not used because interference limited the useful bandwidth to 1.5 MHz, rather than the 4 MHz used elsewhere. Because baseline combinations and the volume of data per source varied form source to source the errors range form 10 to 30 mJy.

4. The new sample of GPS spectrum sources

Finally we merged Subsample One (24 sources) with those 98 sources from Subsample Two whose flux densities we had successfully measured with MERLIN at 408 MHz. Since the selection process for this project was carried out, the 5 GHz Green Bank survey of WB92 has been superseded by the GB6 survey (Gregory et al. 1996) and at 1.4 GHz we can now use the the NRAO VLA Sky Survey (NVSS)[4] (Condon et al. 1998) which has a resolution of 45″ and an rms sensitivity of approximately 1.5 mJy.

[4] available at ftp://nvss.cv.nrao.edu/pub/nvss/CATALOG

Table 2. Subsample Two — flux densities of sources at 408 MHz

IAU name (B1950)	R.A. (J2000)	Dec.	Flux [mJy]	Opt. ID
0001+478	00 03 46.0413	48 07 04.134	104	BS
0015+529	00 17 51.7596	53 12 19.126	100	BS
0046+511	00 49 37.9901	51 28 13.700	123	NS
0051+679	00 54 17.6237	68 11 11.175	127	OB
0051+706	00 54 17.6884	70 53 56.625	260	NS
0058+498	01 01 16.9988	50 04 44.991	125	BS
0102+511	01 05 29.5588	51 25 46.576	262	NS
0123+731	01 27 04.7169	73 23 12.676	330	EF
0129+431	01 32 44.1273	43 25 32.667	244	BS
0129+560	01 32 20.4503	56 20 40.372	113	CW
0140+490	01 43 46.8791	49 15 41.586	105	CW
0148+546	01 51 36.2876	54 54 37.688	100	EF
0153+389	01 56 31.4088	39 14 30.929	119	BS
0213+444	02 16 17.1707	44 37 43.405	154	EF
0251+393	02 54 42.6316	39 31 34.714	114	BS
0307+380	03 10 49.8805	38 14 53.845	148	NS
0335+599	03 39 09.3942	60 08 56.960	134	RS
0336+473	03 40 10.7897	47 32 27.328	103	BS
0338+480	03 42 10.3522	48 09 46.948	113	NS
0412+447	04 15 56.5246	44 52 49.676	110	OB
0424+414	04 27 46.0455	41 33 01.091	272	EF
0454+550	04 58 54.8417	55 08 42.042	192	BS
0513+714	05 19 28.8835	71 33 03.740	153	EF
0514+474	05 18 12.0899	47 30 55.536	220	CW
0533+446	05 37 30.0630	44 41 03.533	155	?
0559+422	06 02 58.9438	42 12 09.999	259	BS
0610+510	06 14 49.1589	51 02 13.124	143	BG
0621+446	06 25 18.2652	44 40 01.628	101	BS
0630+497	06 33 52.2068	49 43 45.939	149	BS
0651+410	06 55 10.0243	41 00 10.148	130	G
0655+696	07 01 06.6159	69 36 29.414	293	BS
0708+742	07 14 36.1236	74 08 10.142	105	BS
0713+669	07 18 05.6314	66 51 53.332	145	EF
0718+374	07 22 01.2600	37 22 28.628	64	BS
0732+755	07 39 13.1962	75 27 47.702	141	EF
0753+373	07 56 28.2513	37 14 55.647	59	BS
0753+519	07 56 59.5457	51 51 00.237	98	BS
0758+594	08 02 24.5932	59 21 34.800	102	BS
0849+675	08 53 34.3220	67 22 15.665	212	BS
0851+719	08 56 54.8695	71 46 23.894	105	BS
0900+520	09 03 58.5758	51 51 00.658	354	?
0924+732	09 29 42.1565	73 04 04.553	114	G
0925+745	09 30 53.7823	74 20 05.930	112	EF
0939+620	09 43 14.5025	61 50 33.343	99	BS
1017+436	10 20 27.2021	43 20 56.342	51	BS
1019+429	10 22 13.1324	42 39 25.618	138	RS
1032+509	10 35 06.0176	50 40 06.087	198	EF
1035+430	10 38 18.1899	42 44 42.766	194	RS
1043+541	10 46 24.0372	53 54 26.220	181	BS
1055+433	10 58 02.9208	43 04 41.505	182	EF
1101+609	11 04 53.6946	60 38 55.287	151	BS
1125+366	11 27 58.8707	36 20 28.352	86	BS
1138+644	11 41 12.2283	64 10 05.484	180	EF

Table 2. continued

IAU name (B1950)	R.A. (J2000)	Dec.	Flux [mJy]	Opt. ID
1157+532	12 00 06.0107	53 00 37.118	188	Q
1206+415	12 09 22.7884	41 19 41.369	152	BS
1226+638	12 29 06.0256	63 35 00.986	153	RS
1232+366	12 35 05.8076	36 21 19.308	121	BS
1239+606	12 41 29.5907	60 20 41.320	136	BS
1245+676	12 47 33.3300	67 23 16.457	107	G
1300+485	13 02 17.1974	48 19 17.572	163	BS
1308+471	13 10 53.5906	46 53 52.219	160	EF
1320+394	13 22 55.6615	39 12 07.984	119	BS
1321+410	13 24 12.0940	40 48 11.773	92	BS
1337+637	13 39 23.7812	63 28 58.425	185	BS
1338+381	13 40 22.9519	37 54 43.839	105	RS
1357+404	13 59 38.0943	40 11 38.260	129	EF
1403+411	14 05 07.7949	40 56 57.847	134	BS
1454+447	14 55 54.1361	44 31 37.668	115	BS
1533+487	15 35 14.6540	48 36 59.697	122	BS
1534+501	15 35 52.0395	49 57 39.084	103	BS
1544+398	15 45 53.2331	39 41 46.857	168	G
1607+563	16 08 20.7518	56 13 56.373	129	BS
1614+466	16 16 03.7667	46 32 25.231	98	BS
1722+611	17 22 40.0578	61 05 59.801	213	BS
1724+609	17 24 41.4142	60 55 55.731	179	EF
1753+648	17 54 07.5904	64 52 02.642	89	BS
1801+459	18 02 25.1427	45 57 34.645	192	BS
1812+560	18 12 57.6692	56 03 49.198	193	BS
1820+397	18 21 59.6991	39 45 59.647	743	BS
1822+682	18 21 59.4951	68 18 43.003	192	BS
1828+399	18 29 56.5203	39 57 34.690	116	EF
1839+389	18 40 57.1550	39 00 45.712	133	BS
1839+548	18 40 57.3780	54 52 15.920	121	BS
1937+630	19 38 16.1680	63 07 17.803	254	?
1939+429	19 40 49.3198	43 04 24.671	197	BS
1941+413	19 42 58.6385	41 29 23.073	167	BS
2000+472	20 02 10.4183	47 25 28.777	150	CW
2005+642	20 06 17.6949	64 24 45.423	137	RS
2013+508	20 14 28.5899	50 59 09.532	174	EF
2014+463	20 15 39.9865	46 28 50.886	122	CW
2112+374	21 14 44.1230	37 42 25.719	181	CW
2119+709	21 19 54.1676	71 10 36.091	147	EF
2151+431	21 53 50.9585	43 22 54.497	110	NS
2202+716	22 03 30.4694	71 51 08.527	200	RS
2248+555	22 50 42.8496	55 50 14.608	212	G
2300+638	23 02 41.3165	64 05 52.858	117	EF
2310+724	23 12 19.6998	72 41 26.924	231	EF
2341+697	23 43 43.7360	70 03 19.398	160	NS

Explanation of ID field is given in Table 1.

Table 3. Subsample Two — sources not measured at 408 MHz

IAU name (B1950)	R.A. (J2000)	Dec.	Opt. ID
0310+435	03 14 08.0539	43 45 19.770	EF
0314+696	03 19 22.0734	69 49 25.603	EF
0418+437	04 21 52.0619	43 53 04.216	CW
0537+392	05 40 44.4377	39 16 12.236	RS
0601+578	06 05 42.2275	57 53 16.351	BS
0638+528	06 42 27.8215	52 47 59.282	BS
0644+491	06 48 47.1190	49 07 20.736	BS
0651+428	06 54 43.5263	42 47 58.728	G
0903+669	09 07 23.5240	66 44 46.942	EF
1238+702	12 40 34.6989	69 58 30.616	BS
1245+716	12 47 09.3270	71 24 20.018	EF
1341+691	13 43 00.5520	68 55 17.160	BS
1406+564	14 08 12.9466	56 13 32.488	BS
1436+445	14 38 28.5048	44 18 12.085	BS
1447+536	14 48 59.1739	53 26 09.282	EF
1456+375	14 58 44.7949	37 20 21.627	BS
1526+670	15 26 42.8732	66 50 54.617	NS
1550+582	15 51 58.2077	58 06 44.466	BS
1611+425	16 13 04.8038	42 23 18.903	BS
1622+665	16 23 04.5221	66 24 01.084	G
1924+420	19 26 31.0504	42 09 58.991	G
2119+664	21 20 46.2045	66 42 20.216	EF
2132+406	21 34 24.1053	40 50 11.345	EF
2230+625	22 32 22.8655	62 49 36.436	OB
2236+678	22 38 15.0284	68 04 59.758	OB
2249+402	22 51 59.7715	40 30 58.155	BS
2351+550	23 53 42.3011	55 18 40.670	BS

Explanation of ID field is given in Table 1.

Unfortunately, at the time of writing, at the time of writin, NVSS — although almost complete — did not cover all areas of the sky within its declination limits. Many NVSS maps ($4^\circ \times 4^\circ$ each) appear to be "patchy" and the "holes" can sometimes be quite large. Our survey suffered considerably from this shortcoming of the current edition of NVSS — 9 sources out of those 122 sources we wanted to study were simply not present in the NVSS catalogue. (One source out of these nine was also unavailable in GB6.) Additionally we decided to remove 2 other sources from the further processing: one of these is blended with a nearby source and the second one has an extended structure which should be studied in more detail.

At 1.4 GHz we also tried to use the Faint Images of Radio Sky at Twenty (FIRST) catalogue[5] (White et al. 1997) — 24 our sources could be found there. For 20 objects out of these we noted a very good compatibility between FIRST and NVSS based fluxes; the 4 objects which showed discrepancy are indicated in Table 6.

The selection process described above gave us finally 111 objects for which we arrayed the flux density values at each frequency. Then we attempted to fit model spectra to the available data using a broken power-law with the following formula (Moffet 1975):

$$S(\nu) = \frac{S_0}{1-\mathrm{e}^{-1}} \cdot (\nu/\nu_0)^k \cdot (1-\mathrm{e}^{-(\nu/\nu_0)^{l-k}}). \quad (2)$$

Here k and l are the spectral indices of the rising and declining parts of the spectrum as often used in radio astronomy, while S_0 and ν_0 are just fitting parameters which are *not* equal to the maximum flux density ($S_{\max}$) and the peak frequency ($\nu_{\max}$) of the fitted spectrum. Even though the broken power-law seems to be the physically more sensible choice for a model spectrum compared to a simple second-order polynomial, it has the disadvantage that it is unconstrained if the peak of the spectrum falls beyond the 2nd highest or below the 2nd lowest available frequency. In these cases we fixed the peak of the model spectrum (i.e. $S_{\max}$ and $\nu_{\max}$) at the peak of the measured data — this was usually the measurement at 4.85 GHz — and marked the fit as unconstrained in Table 4. This means that the values for k or l have to be considered as a lower or upper limit respectively (i.e. in reality the spectrum will be more inverted at low frequencies or steeper at high frequencies).

The spectra of 35 sources could not be fitted with such a convex-shaped curve (Fig. 1) and we claim that those sources cannot be termed "GPS sources" at all and most likely are just variable flat-spectrum sources. The 76 spectra that could be fitted with our algorithm are presented in Fig. 2 and the fitting parameters are given in Table 4. As can be seen from Fig. 2 and Table 4, some of the sources with unconstrained model spectra, fit the data relatively poorly at low frequencies or have relatively flat spectral indices (e.g. 0307+380 and 0610+510) and thus are less probable GPS candidates.

In Table 5 we specified some parameters of our "new" GPS sources gathered from the literature: the names of other catalogues a particular source is a member, the optical identification according to the NASA/IPAC Extragalactic Database (NED) and the redshift. At the time of writing 21 objects from our collection have been identified (3 galaxies[6], 18 QSOs) and their redshifts are known. Those 3 galaxies have low redshifts ($z \lesssim 0.1$); on the other hand — as expected — the majority of quasars have large redshifts: for 6 QSOs $1 < z \lesssim 2$, for 7 other QSOs $z \gtrsim 2$. One QSO, 1338+381, is extremely redshifted: $z = 3.103$.

Most of the GPS sources studied so far hardly show any variability, therefore we checked our sources against possible flux variations. Firstly, because a significant variability of the flux density would mean that the source in question is likely not to be a GPS and secondly —

[5] available at http://sundog.stsci.edu/

[6] It is worth noting that our identifications shown in Tables 1 and 2 yielded 4 galaxies. The identifications for 0651+410 and 1245+676 are given by NED, for the two other ones — 1544+398 and 2248+555 — are not.

Table 4. GPS sources' spectra fitting parameters

Number	B1950name	S_0	ν_0	k	l	$S_{\max}$	$\nu_{\max}$	unconstrained
1	0001+478	286.	3.66	+0.671	−2.1	332.	2.68	
2	0015+529	657.	3.27	+1.13	−0.381	687.	4.82	
3	0046+511	246.	7.14	+0.549	−1.63	284.	4.85	•
4	0051+679	324.	6.97	+0.577	−1.85	379.	4.85	•
5	0058+498	187.	5.94	+0.322	−1.76	237.	3.49	
6	0102+480	1110.	3.03	+1.06	−0.774	1110.	3.01	
7	0102+511	530.	1.85	+0.775	−1.33	564.	1.42	•
8	0123+731	361.	3.25	+0.264	−1.27	449.	1.63	
9	0129+560	659.	3.42	+1.05	−0.956	662.	3.14	
10	0140+490	228.	4.28	+0.524	−1.53	262.	2.85	
11	0148+546	137.	8.39	+0.256	−1.86	181.	4.73	
12	0153+389	203.	7.44	+0.404	−2.17	257.	4.85	•
13	0307+380	581.	6.21	+0.862	−1.66	628.	4.85	•
14	0335+599	192.	7.92	+0.309	−2.12	251.	4.85	•
15	0336+473	295.	2.96	+0.762	−0.886	301.	2.43	
16	0412+447	277.	7.84	+0.349	+0.349			
17	0454+550	257.	7.85	+0.302	−2.23	340.	4.85	•
18	0513+714	219.	3.26	+0.394	−1.19	253.	1.91	
19	0514+474	863.	2.05	+1.13	−0.842	863.	2.02	
20	0610+510	143.	9.9	+0.157	−1.74	198.	4.85	•
21	0627+532	832.	0.767	+0.996	−0.593	835.	0.836	
22	0630+497	183.	7.51	+0.245	−2.89	255.	4.85	•
23	0651+410	408.	6.57	+0.661	−1.06	431.	4.85	•
24	0652+577	528.	0.564	+1.01	−0.649	528.	0.592	
25	0655+696	481.	1.63	+0.69	−0.644	484.	1.42	•
26	0718+374	277.	6.62	+0.692	−1.43	302.	4.85	•
27	0750+535	602.	2.26	+0.57	−1.44	678.	1.55	
28	0753+373	287.	2.85	+1.05	−1.15	292.	2.5	
29	0753+519	221.	3.66	+0.58	−1.22	242.	2.52	
30	0758+594	221.	2.84	+0.635	−0.711	225.	2.27	
31	0849+675	308.	2.72	+0.44	−1.11	347.	1.66	
32	0925+745	284.	4.95	−1.07	+0.554	287.	4.26	
33	1017+436	212.	6.49	+0.728	−2.22	246.	4.85	•
34	1019+429	277.	7.5	+0.496	−1.3	314.	4.85	•
35	1032+509	180.	7.71	+0.124	−1.16	245.	2.81	
36	1055+433	267.	0.69	+1.44	−0.237	308.	1.42	•
37	1107+485	712.	0.69	+0.645	−0.845	734.	0.528	
38	1125+366	70.4	0.347	+0.292	+2.14			
39	1138+644	228.	9.59	+0.192	−1.68	307.	4.85	•
40	1206+415	449.	10.4	−2.04	+0.475	492.	7.29	
41	1226+638	422.	2.89	+0.751	−1.24	446.	2.21	
42	1232+366	198.	8.41	+0.372	−1.29	234.	4.85	•
43	1239+606	435.	1.41	+1.31	−0.93	435.	1.42	•
44	1245+676	258.	1.16	+1.29	−0.561	264.	1.42	•
45	1256+546	1090.	0.539	+0.901	−0.925	1110.	0.471	
46	1311+552	1980.	0.555	+1.33	−0.851	1980.	0.578	
47	1321+410	476.	2.83	+1.09	−0.98	478.	2.62	
48	1338+381	330.	3.27	+0.771	−1.21	347.	2.53	
49	1357+404	356.	12.1	+0.349	+0.349			
50	1403+411	223.	6.71	+0.346	−1.58	276.	3.92	

Table 4. continued

Number	B1950name	S_0	ν_0	k	l	$S_{\max}$	$\nu_{\max}$	unconstrained
51	1454+447	206.	2.36	+0.588	−0.407	206.	2.43	
52	1532+680	455.	2.57	+0.329	−1.32	551.	1.42	•
53	1534+501	341.	6.97	+0.584	−1.09	367.	4.85	•
54	1544+398	221.	6.4	+0.363	−4.67	310.	4.85	•
55	1607+563	261.	3.54	+0.538	−0.797	273.	2.48	
56	1627+476	219.	3.06	+0.241	−1.11	271.	1.42	•
57	1630+358	466.	2.5	+0.377	−1.11	537.	1.42	•
58	1745+670	548.	2.7	+0.266	−1.46	696.	1.42	•
59	1753+648	220.	7.26	+0.519	−1.66	257.	4.85	•
60	1755+578	785.	2.07	+1.06	−1.07	793.	1.86	
61	1801+459	231.	2.78	+0.337	−0.77	256.	1.46	
62	1815+614	580.	3.9	+0.0731	−1.69	852.	1.61	
63	1820+397	753.	0.457	−0.519	+0.527	761.	0.575	
64	1839+548	240.	5.62	+0.436	−0.983	265.	3.42	
65	1946+708	965.	1.92	+0.818	−0.755	970.	1.72	
66	2000+472	946.	4.11	+0.996	−0.588	949.	4.51	
67	2005+642	227.	0.502	+0.346	+3.4			
68	2013+508	363.	1.67	+0.849	−0.927	369.	1.42	•
69	2014+463	153.	8.03	+0.231	−1.88	205.	4.44	
70	2119+709	167.	9.07	+0.217	−1.79	224.	4.85	•
71	2151+431	257.	3.25	+0.63	−0.917	268.	2.41	
72	2248+555	469.	4.72	+0.512	−0.633	481.	3.43	
73	2253+417	1840.	1.83	+0.706	−0.909	1900.	1.44	
74	2310+385	682.	3.2	+0.6	−1.14	735.	2.25	
75	2341+697	155.	7.5	+0.147	−1.59	213.	3.45	
76	2356+385	560.	3.85	+0.524	−1.34	632.	2.55	

since our data are not simultaneous — any variability makes derivation of spectra questionable. The part of sources' spectra around 1.4 GHz is obviously the most "sensitive" with regard to the GPS phenomenon so we compared fluxes at this frequency given in WB92 to those from NVSS. We applied corrections for the different beam sizes of these two measurements. If a particular source had changed its flux between epochs of the GB surveys and NVSS/FIRST more than 25% or the 1.4 GHz GB flux was missing in WB92 we treated such a source as potentially variable, unless we could find a second epoch flux density measurement elsewhere. We assigned a "candidate" status for such objects and listed them in Table 6. Among these there are 4 sources (0412+447, 1125+366, 1357+404, 2005+642) with inverted spectra only, i.e. apparently having turnovers in their spectra at frequencies larger than 8.4 GHz. This feature was yet another reason to assign them a candidate status.

5. Notes on individual sources

Apart from the information in Table 5 we note that:

- 0627+532, 0652+577, 1107+485, 1256+546 and 1311+552 are 6C sources (Hales et al. 1993 and references therein).
- 1107+485 is a member of the DRAO 408 MHz survey (Green & Riley 1995).
- 1745+670 and 1753+648 are members of the NEP survey (Kollgaard et al. 1994).
- 1607+563, 1755+578 and 1815+614 are members of the 7C survey (Visser et al. 1995).
- 0514+474 was observed by Leahy & Roger (1996).
- 0102+480 and 2253+417 are members of the CJ1 survey (Polatidis et al. 1995).
- 1245+676 is a giant radio galaxy with a GPS core (O'Dea priv. comm. 1996).
- 0140+490 has a large scale symmetric structure 2.″5 across.
- 1839+548 and 2119+709 are marked as "quasi-point" sources in JVAS. All other sources are pointlike i.e. they are unresolved by the VLA in "A" configuration at 8.4 GHz.
- 1815+614 and 1946+708 are CSOs (Taylor et al. 1996; Taylor & Vermeulen 1997).

6. Summary

Gigahertz Peaked Spectrum objects are an astrophysically significant and important class yet they are still not well understood (O'Dea 1998). They are not necessarily a uniform class, and one can easily name subclasses among the whole GPS ensemble. For example CSOs make one well defined group — all of them are GPS galaxies with characteristic VLBI morphologies. It is claimed by Readhead

Table 5. Some other parameters of JVAS GPS sources

Number	B1950name	S4/S5	FIRST	B3	WENSS	CJ2	Opt. ID	z	Redshift reference
1	0001+478								
2	0015+529								
3	0046+511								
4	0051+679								
5	0058+498								
6	0102+480	•							
7	0102+511								
8	0123+731	•							
9	0129+560								
10	0140+490								
11	0148+546								
12	0153+389								
13	0307+380			•		•	QSO	0.816	Vermeulen & Taylor, 1995
14	0335+599								
15	0336+473								
16	0412+447								
17	0454+550								
18	0513+714								
19	0514+474			•					
20	0610+510						QSO	1.59	Hook et al., 1996
21	0627+532	•				•	QSO	2.204	Henstock et al., 1997
22	0630+497	•							
23	0651+410					•	G	0.02156	Marzke et al., 1996
24	0652+577								
25	0655+696						QSO	1.971	Moran et al., 1996
26	0718+374		•						
27	0750+535		•						
28	0753+373		•						
29	0753+519		•				QSO	1.33	Hook et al., 1996
30	0758+594								
31	0849+675								
32	0925+745	•							
33	1017+436		•				QSO	1.96	Hook et al., 1996
34	1019+429	•	•	•					
35	1032+509		•						
36	1055+433	•	•	•					
37	1107+485	•	•				QSO	0.74	Hook et al., 1996
38	1125+366		•						
39	1138+644								
40	1206+415		•			•			
41	1226+638								
42	1232+366	•	•				QSO	1.60	Hook et al., 1996
43	1239+606								
44	1245+676						G	0.103	Marzke et al., 1996
45	1256+546		•						
46	1311+552	•	•			•	QSO	0.613	Vermeulen et al., 1996
47	1321+410	•	•			•	QSO	0.496	Vermeulen et al., 1996
48	1338+381	•	•				QSO	3.103	Hook et al., 1995
49	1357+404		•						
50	1403+411		•	•					

Table 5. continued

Number	B1950name	S4/S5	FIRST	B3	WENSS	CJ2	Opt. ID	z	Redshift reference
51	1454+447		•						
52	1532+680				•				
53	1534+501	•	•			•	QSO	1.119	Vermeulen & Taylor, 1995
54	1544+398	•	•	•					
55	1607+563		•						
56	1627+476		•						
57	1630+358		•						
58	1745+670				•				
59	1753+648				•				
60	1755+578	•			•	•	QSO	2.110	Henstock et al., 1997
61	1801+459			•					
62	1815+614				•	•	QSO	0.601	Vermeulen & Taylor, 1995
63	1820+397	•		•					
64	1839+548								
65	1946+708	•			•	•	G	0.101	Stickel & Kühr, 1993
66	2000+472								
67	2005+642				•	•	QSO	1.574	Henstock et al., 1997
68	2013+508								
69	2014+463								
70	2119+709								
71	2151+431								
72	2248+555								
73	2253+417	•					QSO	1.476	Hewitt & Burbidge, 1989
74	2310+385					•	QSO	2.17	Hewitt & Burbidge, 1989
75	2341+697								
76	2356+385	•				•	QSO	2.704	Stickel & Kühr, 1994

References of the catalogues:

S4 — Pauliny-Toth et al., 1978.
S5 — Kühr et al., 1981b.
FIRST — White et al., 1997.
B3 — Ficarra et al., 1985.
WENSS — Rengelink et al., 1997.
CJ2 — Taylor et al., 1994.

et al. (1996b) that CSOs play a key role as an initial stage in the evolutionary scenario of radio-loud AGNs.

Another fascinating subset of GPS class are objects with extreme ($z > 3$) redshifts. There are 9 such objects in the "working sample" (O'Dea, priv. comm. 1996). Additionally there are ∼20 objects with high ($1 < z < 3$) redshifts. All the objects with $z > 1$ are identified with quasars.

The above two issues alone are already a good argument to extend the number of known GPS radio sources. With such a goal in mind we have made a search for candidate GPS sources in the part of the Jodrell Bank–VLA Astrometric Survey limited to $35° \leq \delta \leq 75°$, namely we compared 8.4 GHz flux densities derived from JVAS with respective 1.4 GHz and 5 GHz fluxes in available catalogues. We treated a source as a plausible candidate if its spectrum seemed to be convex according to the criterion we had arbitrarily assumed.

Quite expectedly some of the candidates selected in this manner are already recognised as GPS objects so we did not deal with them here. Using flux densities at low frequencies i.e. 365 MHz and sometimes even 151 MHz in available catalogues we were able to classify 24 objects as GPS sources without any further measurements. For the majority of selected objects the flux densities at frequencies well below 1 GHz were not available. In these cases we performed observations with MERLIN at 408 MHz to establish the low-frequency part of the spectra.

Our final decision on which of our candidates are and which are not GPS sources has been made based on our MERLIN data (or Texas catalogue when available), NVSS, GB6 and JVAS catalogues. Combining flux density measurements made with high resolution both at low (MERLIN, 408 MHz) and high (VLA, 8.4 GHz) frequencies enabled us to eliminate the effects of confusion and any contribution from possible extended "halos".

Table 6. Candidate GPS sources

B1950name	Reason
0001+478	GB flux is 73% greater than NVSS flux
0046+511	no 2nd epoch data
0051+679	GB flux is 36% greater than NVSS flux
0058+498	no 2nd epoch data
0307+380	poor fit to the broken power-law curve
0412+447	GB flux is 4.7 times greater than NVSS flux, inverted spectrum only
0651+410	no 2nd epoch data
0655+696	GB flux is 55% less than NVSS flux
0718+374	no 2nd epoch data
0753+519	no 2nd epoch data
0758+594	GB flux is 34% less than NVSS flux
1017+436	no 2nd epoch data
1055+433	B3 flux (420 mJy) and MERLIN 408 MHz flux (182 mJy) do not match
1125+366	FIRST flux does not match NVSS and GB fluxes, inverted spectrum only
1206+415	FIRST flux does not match NVSS and GB fluxes
1232+366	FIRST flux matches NVSS flux but they both don't match GB and S4 fluxes — extended component?
1357+404	FIRST flux does not match NVSS and GB fluxes, inverted spectrum only
1544+398	B3 flux matches MERLIN flux but FIRST flux does not match NVSS and GB fluxes
1839+548	no 2nd epoch data
2005+642	inverted spectrum only
2013+508	GB flux is 48% less than NVSS flux
2014+463	no 2nd epoch data
2248+555	no 2nd epoch data
2341+697	no 2nd epoch data

We regarded a source as a GPS if it had fitted well a "broken power-law" function and was not variable.

The sample we present here is the largest single contribution to the pool of known GPS sources collected so far. Only 3 of our sources (0513+714, 0758+594, 1946+708) are overlapping with another large collection of GPS sources, namely with the WENSS based sample[7] (SSB98). Seven sources in our sample have large redshifts ($z \gtrsim 2$); the largest one is $z = 3.103$.

Our approach to finding GPS sources was to search from high frequency to lower ones. WENSS has been equally successful in defining GPS sources but searching from low frequencies to higher ones. We want to stress though that our approach can successfully be applied to the areas of the sky *not* planned to be covered by WENSS ($\delta < 30^\circ$) but already covered by the other catalogues we used (NVSS, GB6, JVAS). For the part of JVAS we used so far (Patnaik et al. 1992) we found that 9% of JVAS sources are GPS; therefore the whole JVAS encompassing around 3000 sources could easily yield $250 - 300$ of such objects.

[7] 0513+714 and 0758+594 are not marked in Table 5 as WENSS sources because these objects are not mentioned by Rengelink et al. (1997). On the other hand, except 1946+708, the WENSS objects we list in Table 5 have *not* been recognised as GPS by SSB98.

Acknowledgements. The initial stages of the programme described in this paper were completed when AM stayed at MPIfR in Bonn. The Max-Planck-Gesellschaft stipend which supported him in that time is gratefully acknowledged.

AM acknowledges support from the Polish State Committee for Scientific Research grant 2.P304.003.07 and EU grant ERBCIPDCT940087.

HF is supported in part by the DFG, grant Fa 358/1-1&2.

We thank the NVSS team led by Jim Condon for making NVSS public domain data prior its final publication. Special thanks to Bill Cotton for his co-operation.

This research has made use of the NASA/IPAC Extragalactic Database (NED) which is operated by the Jet Propulsion Laboratory, California Institute of Technology, under contract with the National Aeronautics and Space Administration.

References

Baars J.W.M., Genzel R., Pauliny-Toth I.I.K., Witzel A., 1977, A&A 61, 99

Cersosimo J.C., Lebron Santos M., Cintrón S.I., Quiniento Z.M., 1994, ApJS 95, 157

Condon J.J., Cotton W.D., Greisen E.W., et al., 1998, AJ 115, 1693

Douglas J.N., Bash F.N., Arakel Bozyan F., Torrence G.W., 1996, AJ 111, 1945

Ficarra A., Grueff G., Tomasetti G., 1985, A&AS 59, 255

Gopal-Krishna, Patnaik A.R., Steppe H., 1983, A&A 123, 107

Gopal-Krishna, Spoelstra T.A.Th., 1993, A&A 271, 103
Green D.A., Riley J.M., 1995, MNRAS 274, 324
Gregory P.C., Scott W.K., Douglas K., Condon J.J., 1996, ApJS 103, 427
Hales S.E.G., Baldwin J.E., Warner P.J., 1993, MNRAS 263, 25
Henstock D.R., Browne I.W.A., Wilkinson P.N., McMahon R.G., 1997, MNRAS 290, 380
Hewitt A., Burbidge G., 1989, magnetic tape
Hook I.M., McMahon R.G., Patnaik A.R., et al., 1995, MNRAS 273, 63
Hook I.M., McMahon R.G., Irwin M.J., Hazard C., 1996, MNRAS 282, 1274
Kollgaard R.I., Brinkmann W., McMath Chester M., et al., 1994, ApJS 93, 145
Kühr H., Witzel A., Pauliny-Toth I.I.K., Nauber U., 1981a, A&AS 45, 367
Kühr H., Pauliny-Toth I.I.K., Witzel A., Schmidt J., 1981b, AJ 86, 854
Leahy D.A., Roger R.S., 1996, A&AS 115, 345
Marzke R.O., Huchra J.P., Geller M.J., 1996, AJ 112, 1803
Moffet A.T., 1975, in: Sandage A., Sandage M., Kristian J. (eds.) Stars and Stellar Systems, Vol. IX, p. 211
Moran E.C., Helfand D.J., Becker R.H., White R.L., 1996, ApJ 461, 127
O'Dea C.P., Baum S.A., Stanghellini C., 1991, ApJ 380, 66 (OBS91)
O'Dea C.P., 1998, PASP 110, 493
Patnaik A.R., Browne I.W.A., Wilkinson P.N., Wrobel J.M., 1992, MNRAS 254, 655
Pauliny-Toth I.I.K., Witzel A., Preuss E., et al., 1978, AJ 83, 451
Polatidis A.G., Wilkinson P.N., Xu W., et al., 1995, ApJS 98, 1
Rengelink R.B., Tang Y., de Bruyn A.G., et al., 1997, A&A 124, 259
Readhead A.C.S., Taylor G.B., Xu W., et al., 1996a, ApJ 460, 612
Readhead A.C.S., Taylor G.B., Pearson T.J., Wilkinson P.N., 1996b, ApJ 460, 634
Snellen I.A.G., Zhang M., Schilizzi R.T., et al., 1995, A&A 300, 359
Snellen I.A.G., Schilizzi R.T., de Bruyn A.G., et al., 1998, A&AS 131, 435 (SSB98)
Spoelstra T.A.Th., Patnaik A.R., Gopal-Krishna, 1985, A&A 152, 38
Stanghellini C., O'Dea C.P., Baum S.A., Fanti R., 1990, Compact Steep Spectrum & Gigahertz-Peaked Spectrum Sources, Dwingeloo Workshop, 18–19 June 1990, Fanti C., Fanti R., O'Dea C.P., Schilizzi R.T. (eds.)
Stanghellini C., Dallacasa D., O'Dea C.P., et al., 1996, 2nd workshop on GPS and CSS Radio Sources, Leiden, 30 Sept. — 2 Oct. 1996, Snellen I.A.G., Schilizzi R.T., Röttgering H.J.A., Bremer M.N. (eds.)
Stickel M., Kühr H., 1993, A&AS 100, 395
Stickel M., Kühr H., 1994, A&AS 105, 67
Taylor G.B., Vermeulen R.C., 1997, ApJ 485, 9
Taylor G.B., Vermeulen R.C., Pearson T.J., et al., 1994, ApJS 95, 345
Taylor G.B., Vermeulen R.C., Readhead A.C.S., et al., 1996, 2nd workshop on GPS and CSS Radio Sources, Leiden, 30 Sept. — 2 Oct. 1996, Snellen I.A.G., Schilizzi R.T., Röttgering H.J.A., Bremer M.N. (eds.)
Vermeulen R.C., Taylor G.B., 1995, AJ 109, 1983
Vermeulen R.C., Taylor G.B., Readhead A.C.S., Browne I.W.A., 1996, AJ 111, 1013
Visser A.E., Riley J.M., Röttgering H.J.A., Waldram E.M., 1995, A&AS 110, 419
de Vries W.H., Barthel P.D., O'Dea C.P., 1997, A&A 321, 105
Walker R.C., 1981, AJ 86, 1323
Wilkinson P.N., Polatidis A.G., Readhead A.C.S., Xu W., Pearson T.J., 1994, ApJ 432, L87
White R.L., Becker R.H., 1992, ApJS 79, 331 (WB92)
White R.L., Helfand D.J., Becker R.H., Gregg M.D., 1997, ApJ 475, 479

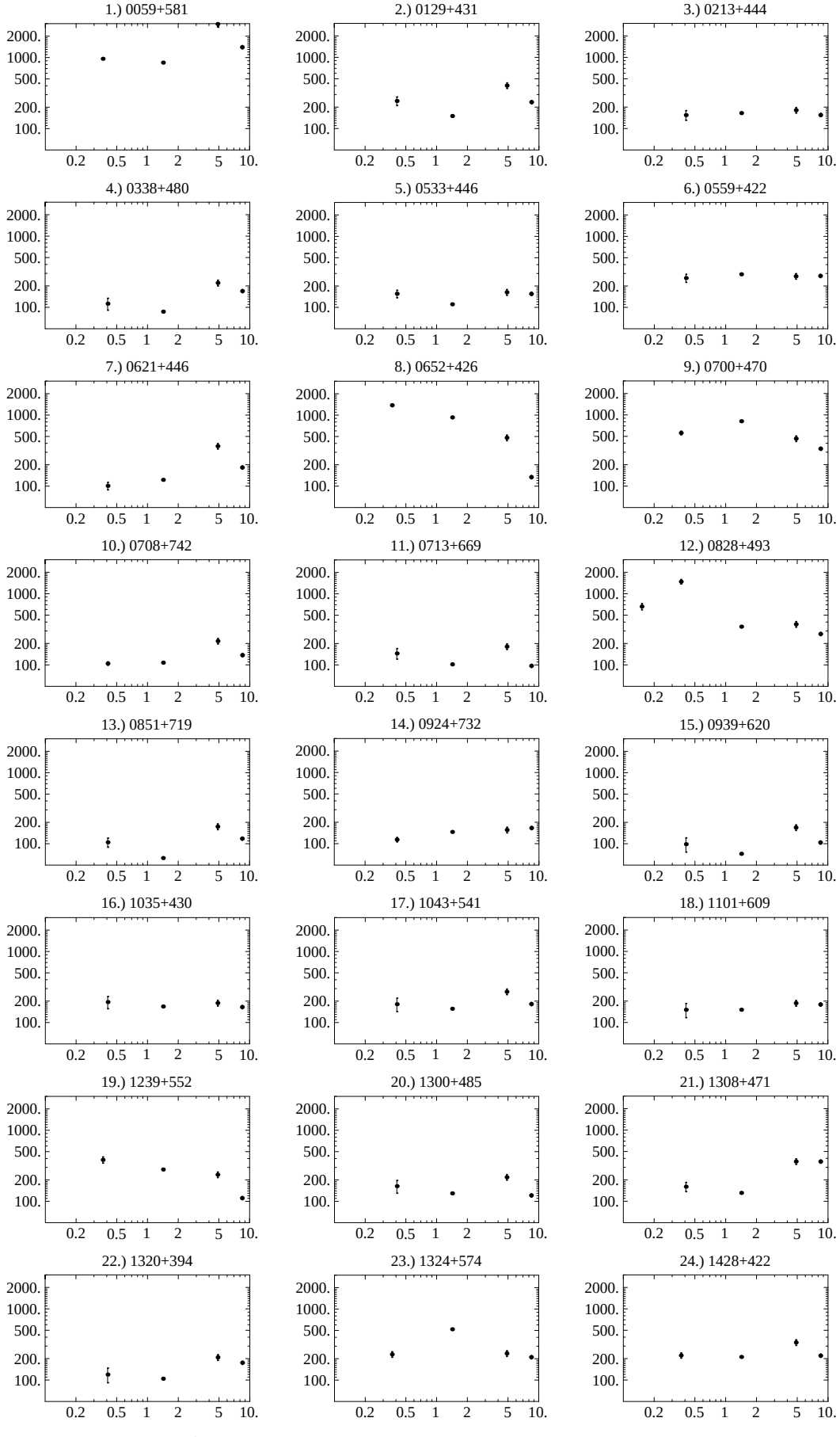

Fig. 1. Spectra of non-GPS sources. Abscissae: frequency in GHz, ordinates: flux densities in mJy

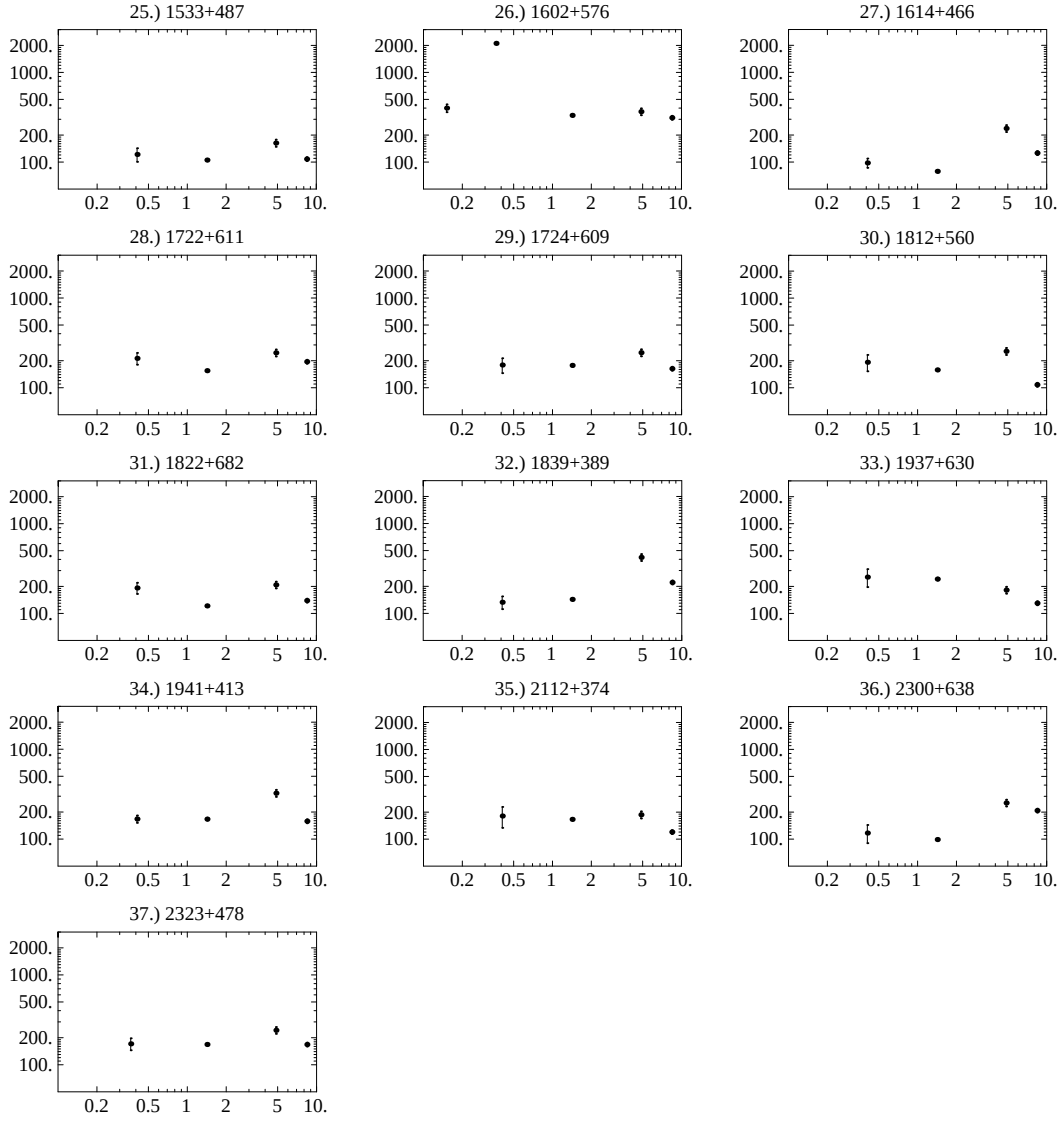

Fig. 1. continued

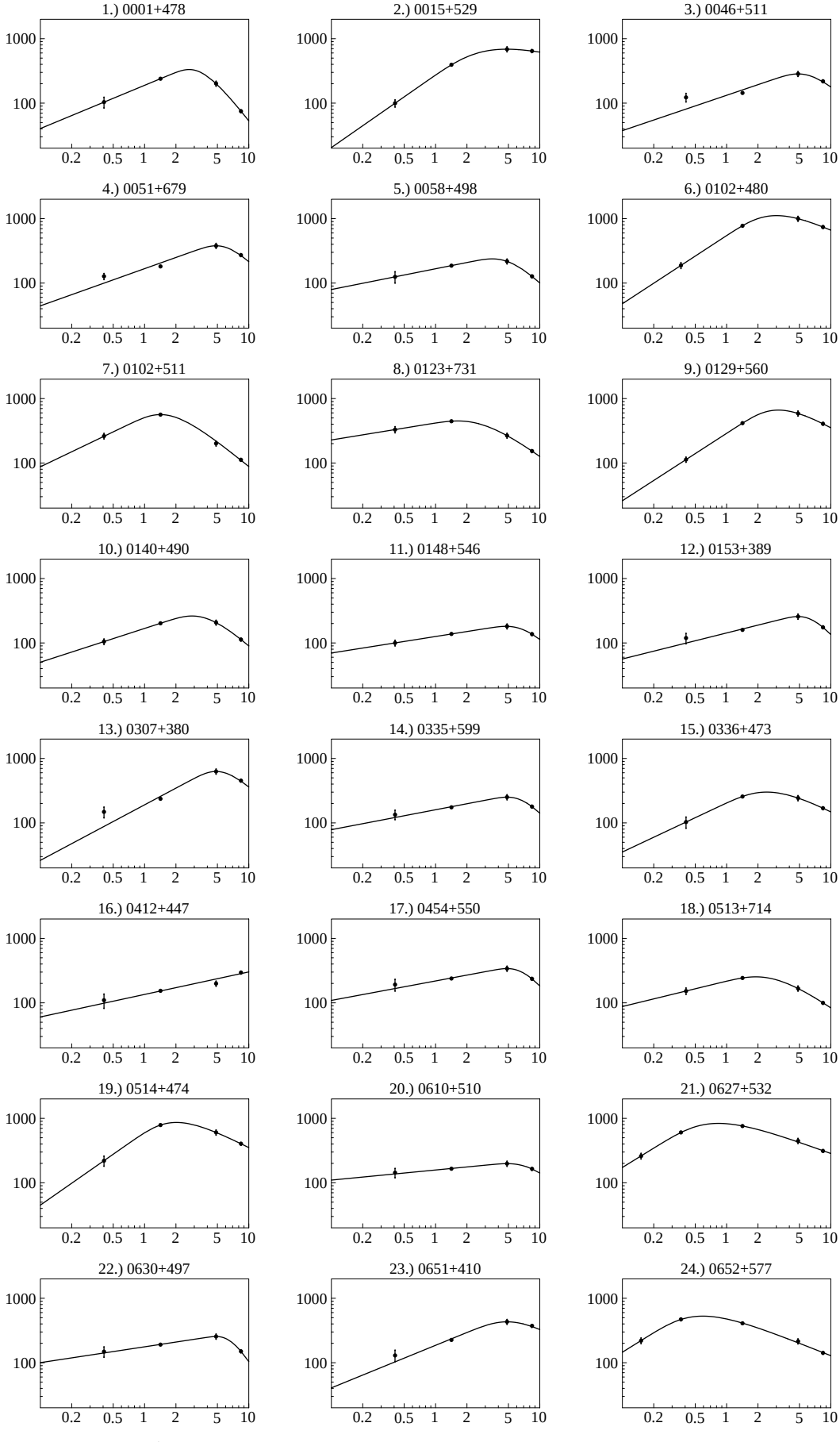

Fig. 2. Spectra of GPS sources. Abscissae: frequency in GHz, ordinates: flux densities in mJy

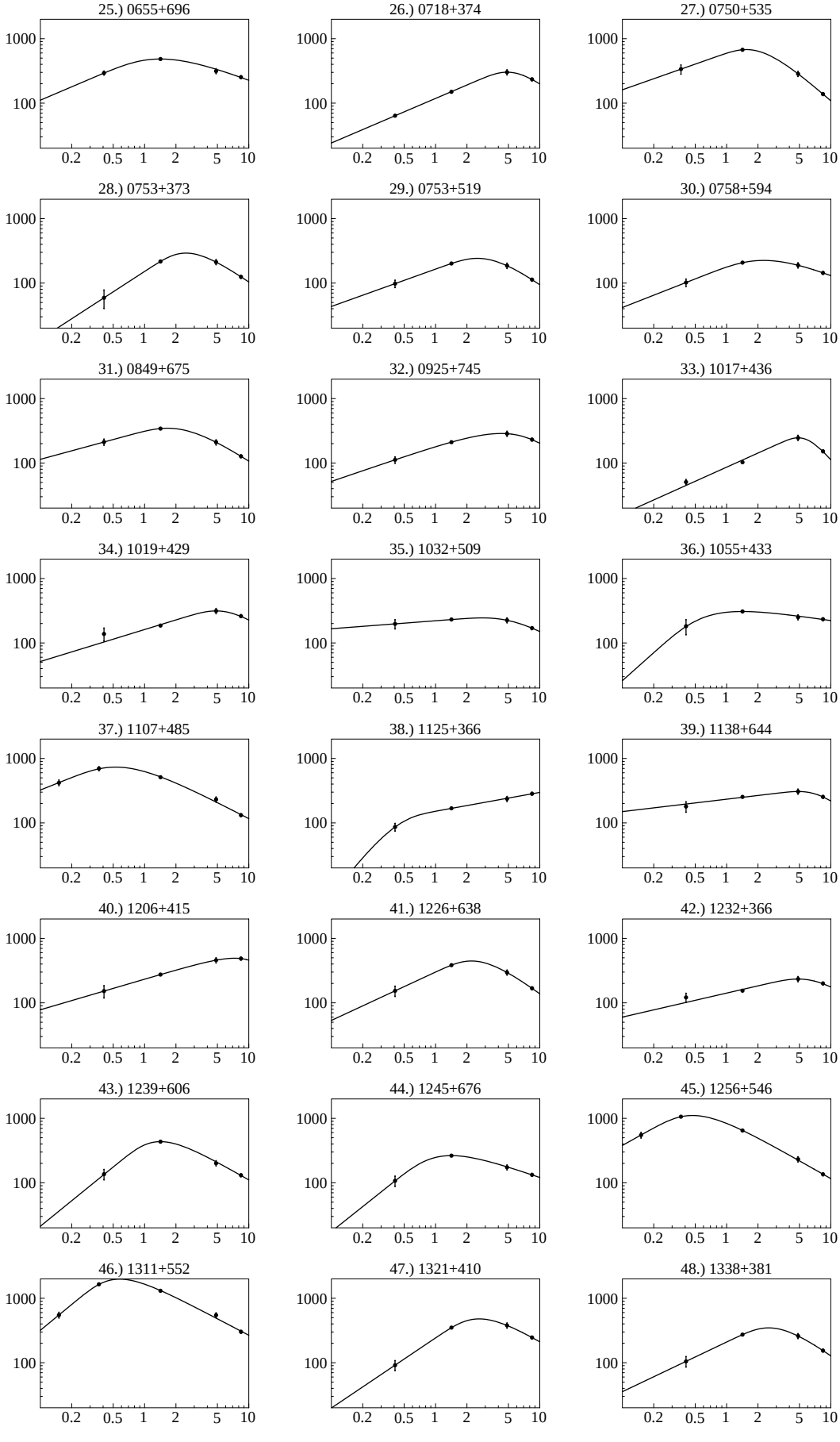

Fig. 2. continued

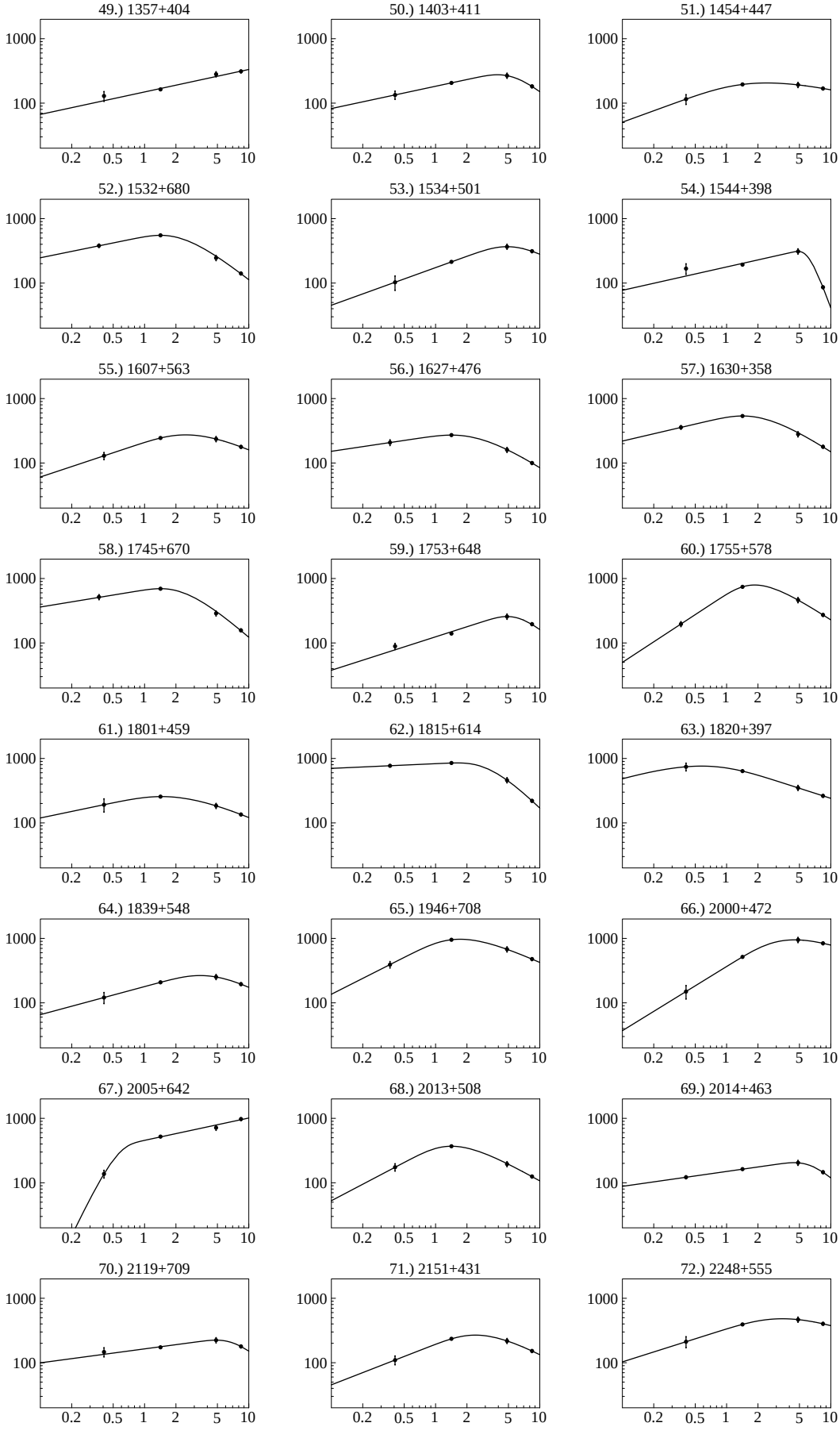

Fig. 2. continued

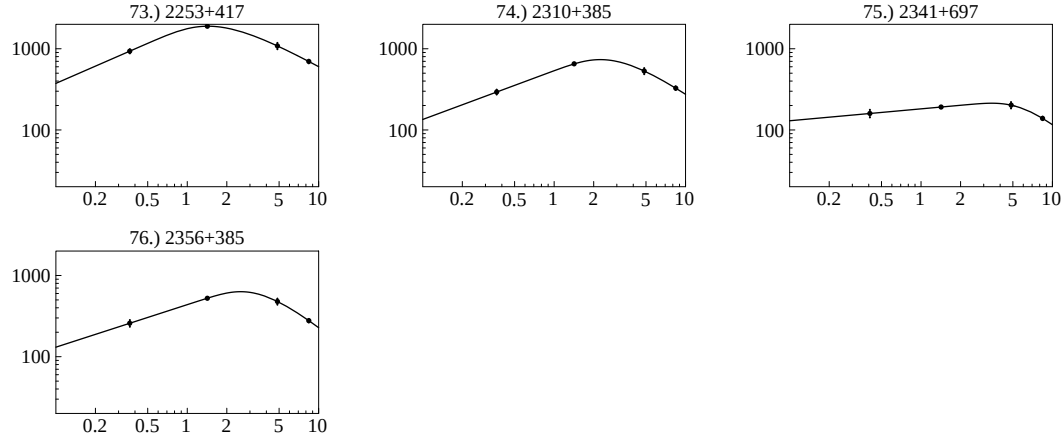

Fig. 2. continued